

# Universal Model of Finite-Reynolds Number Turbulent Flow in Channels and Pipes

Victor S. L'vov, Itamar Procaccia and Oleksii Rudenko

*Department of Chemical Physics, The Weizmann Institute of Science, Rehovot 76100, Israel*

In this Letter we suggest a simple and physically transparent analytical model of pressure driven turbulent wall-bounded flows at high but finite Reynolds numbers  $Re$ . The model provides an accurate quantitative description of the profiles of the mean-velocity and Reynolds-stresses (second order correlations of velocity fluctuations) throughout the entire channel or pipe, for a wide range of  $Re$ , using only three  $Re$ -independent parameters. The model sheds light on the long-standing controversy between supporters of the century-old log-law theory of von-Kàrmàn and Prandtl and proposers of a newer theory promoting power laws to describe the intermediate region of the mean velocity profile.

An important challenge in wall-bounded Newtonian turbulence is the description of the profiles of the mean velocity and second order correlation functions of turbulent-velocity fluctuations throughout the entire channel or pipe at relatively high but finite Reynolds numbers. To understand the issue, focus on a channel of width  $2L$  between its parallel walls, where the incompressible fluid velocity  $\mathbf{U}(\mathbf{r}, t)$  is decomposed into its average (over time) and a fluctuating part

$$\mathbf{U}(\mathbf{r}, t) = \mathbf{V}(\mathbf{r}) + \mathbf{u}(\mathbf{r}, t), \quad \mathbf{V}(\mathbf{r}) \equiv \langle \mathbf{U}(\mathbf{r}, t) \rangle$$

. In a stationary plane channel flow with a constant pressure gradient  $p' \equiv -\partial p/\partial x$  the only component of the mean velocity  $\mathbf{V}$  is the stream-wise component  $V_x \equiv V$  that depends on wall normal direction  $z$  only. Near the wall the mean velocity profiles for different Reynolds numbers exhibit data collapse once presented in wall units, where the Reynolds number  $Re_\tau$ , the normalized distance from the wall  $z^+$  and the normalized mean velocity  $V^+(z^+)$  are defined (for channels) by

$$Re_\tau \equiv L\sqrt{p'L}/\nu, \quad z^+ \equiv zRe_\tau/L, \quad V^+ \equiv V/\sqrt{p'L}$$

. The classical theory of Prandtl and von-Kàrmàn for infinitely large  $Re_\tau$  is based on the assumption that the single characteristic scale in the problem is proportional to the distance from the (nearest) wall. It leads to the celebrated von-Kàrmàn log-law [1]

$$V^+(z^+) = \kappa^{-1} \ln(z^+) + B, \quad (1)$$

which serves as a basis for the parametrization of turbulent flows near a wall in many engineering applications. On the face of it this law agrees with the data (see, e.g. Fig. 1) for relatively large  $z^+$ , say for  $z^+ > 100$ , giving  $\kappa \sim 0.4$  and  $B \sim 5$ . The range of validity of the log-law is definitely restricted by the requirement  $\zeta \ll 1$ , where  $\zeta \equiv z/L$  (channel) or  $\zeta \equiv r/R$  (Pipe of radius  $R$ ). For  $\zeta \sim 1$  the global geometry becomes important leading to unavoidable deviations of  $V^+(\zeta)$  from the log-law (1), known as *the wake*.

The problem is that for finite  $Re_\tau$  the corrections to the log-law (1) are in powers of  $\varepsilon \equiv 1/\ln Re_\tau$  [5] and

definitely cannot be neglected for the currently largest available direct numerical simulation (DNS) of channel flows ( $Re_\tau = 2003$  [3], giving  $\varepsilon \approx 0.13$ ). Even for  $Re_\tau$  approaching 500,000 as in the Princeton Superpipe experiment [4],  $\varepsilon \approx 0.08$ . This opens a Pandora box with various possibilities to revise the log-law (1) and to replace it, as was suggested in [5], by a power law

$$V^+(z^+) = C(Re_\tau)(z^+)^{\gamma(Re_\tau)}. \quad (2)$$

Here both  $C(Re_\tau)$  and  $\gamma(Re_\tau)$  were represented as asymptotic series expansions in  $\varepsilon$ . The relative complexity of this proposition compared to the simplicity of Eq. (1) resulted in a less than enthusiastic response in the fluid mechanics community [6], leading to a rather fierce controversy between the log-law camp and the power-law camp. Various attempts [4–9] to validate the log-law (1) or the alternative power-law (2) were based on extensive analysis of experimental data used to fit the velocity profiles as a formal expansion in inverse powers of  $\varepsilon$  or as composite expansions in both  $z^+$  and  $\zeta$ . Note however that in the excellent fits presented, say in [9], one uses four adjustable parameters for each function.

In this Letter we propose a complementary approach to this issue which will finally use only three  $Re_\tau$ -independent *universal* parameters which will be used for all the functions discussed. First we ask what could be missed in the textbook derivations of the classical log-law (1) which may lead to different velocity profile [including possibly the power law (2)]? Our answer is: the mean turbulent velocity profile in the entire channel or pipe can be described within the traditional approach if one realizes how the characteristic length-scale, which has physical meaning of the size of energy containing eddies  $\ell$ , depends on the position in the flow. Simple scaling near the wall,  $\ell^+ = \kappa z^+$ , leads to the log-law (1). The alternative suggestion of [5],  $\ell^+ \propto (z^+)^{\alpha(Re_\tau)}$ , leads to alternative power-law (2). We see no physical reason why  $\ell$  should behave in either manner. Instead, we propose that the eddy size  $\ell$  should be about  $z$  for  $z \ll L$ , and saturate at some level  $\ell_s \lesssim L$  approaching the centerline, where the effect of the opposite wall is felt. Our analysis of DNS data provides a strong support to this

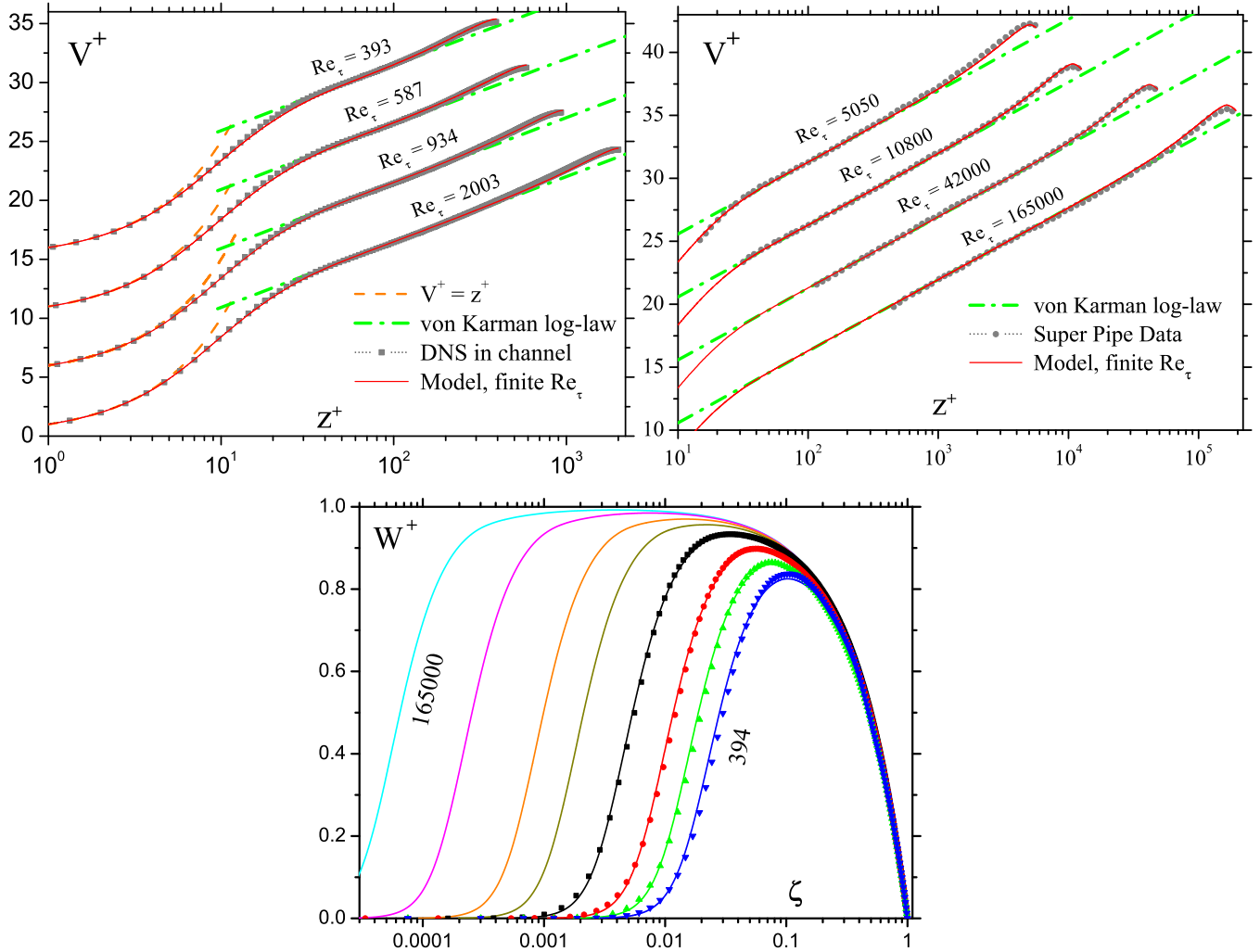


FIG. 1: Color online. **Left and Right upper panels:** comparison of the theoretical mean velocity profiles (red solid lines) at different values of  $Re_\tau$  with the DNS data for the channel flow [2, 3] (Left panel, grey squares; model with  $\ell_{\text{buf}} = 49$ ,  $\kappa = 0.415$ ,  $\ell_s = 0.311$ ) and with the experimental Super-Pipe data [4] (middle panel, grey circles; model with  $\ell_{\text{buf}} = 46$ ,  $\kappa = 0.405$ ,  $\ell_s = 0.275$ ). In orange dashed line we plot the viscous solution  $V^+ = z^+$ . In green dashed dotted line we present the von-Kàrmàn log-law. Note that the theoretical predictions with three  $Re_\tau$ -independent parameters fits the data throughout the channel and pipe, from the viscous scale, through the buffer layer, the log-layer and the wake. For clarity the plots are shifted vertically by five units. **Lower panel:** The Reynolds-stress profiles (solid lines) at  $Re_\tau$  from 394 to 2003 (in channel) and from 5050 to 165,000 (in pipe) in comparison with available DNS data (dots) for the channel.

idea, allowing us to get, within the traditional (second-order) closure procedure, a quantitative description of the mean shear,  $S(z) = dV(z)/dz$ , the kinetic energy density (per unit mass),  $K(z) \equiv \langle |\mathbf{u}|^2 \rangle / 2$ , and the tangential Reynolds stress,  $W(z) \equiv -\langle u_x u_z \rangle$ , in the entire flow and in a wide region of  $Re_\tau$ , using only three  $Re_\tau$ -independent parameters,  $\kappa$ ,  $B$  and  $\ell_s$  ( $\ell_s \approx 0.311 L$  for the channel and  $\ell_s \approx 0.275 L$  for the pipe).

**The closure model** should relate three objects:  $S^+$ ,  $K^+$  and  $W^+$ . The first (exact) relation between these objects follows from the Navier-Stokes equation for the mean velocity, being the mechanical balance between the momentum generated at distance  $z$  from the wall, i.e.  $p'(L-z)$ , and the momentum transferred to the wall by

kinematic viscosity and turbulent transport. In physical and wall units it has the form:

$$\nu S + W = p'(L-z) \Rightarrow S^+ + W^+ = 1 - \zeta, \quad \zeta \equiv z/L. \quad (3)$$

Already in 1877 Boussinesq attempted to close this equation by introducing the notion of turbulent viscosity  $\nu_T$ , writing  $W = \nu_T S$  [10]. Estimating  $\nu_T$  as  $\kappa_w \ell_w \sqrt{K}$ , one finishes with the closure  $W^+ = \kappa_w \ell_w^+ \sqrt{K^+} S^+$ . Here  $\ell_w$  is a  $\zeta$ -dependent characteristic scale of energy containing eddies, determining the nonlinear dissipation of  $W$ , and  $\kappa_w$  is a constant introduced here for convenience. A more careful analysis of the balance equation for  $W$  (see Ref. [11] and Appendix) that includes the viscous dissipation of  $W$ , leads to a somewhat more involved clo-

sure for  $W$  in a form involving an additional *universal*,  $\text{Re}_\tau$ -independent dimensionless function of  $z^+$ :

$$r_w W^+ \approx \kappa_w \ell_w^+ \sqrt{K^+} S^+, \quad r_w(z^+) \equiv \left(1 + \frac{\ell_{\text{buf}}^+{}^6}{z^+{}^6}\right)^{1/6}. \quad (4)$$

Here  $\ell_{\text{buf}}^+ \approx 49$  is a  $\text{Re}_\tau$ -independent length that plays a role of the crossover scale (in wall units) between the buffer and log-law region. In this form,  $\ell_w(\zeta) \propto z$  near the wall, and the choice  $\kappa_w \approx 0.20$  ensures that  $\lim_{\zeta \rightarrow 0} \ell_w(\zeta) = \zeta$ .

A third relation to supplement Eqs. (3) and (4) is obtained by balancing the turbulent energy generated by the mean flow at a rate  $SW$ , and the dissipation at a rate  $\varepsilon_K \equiv \nu \langle |\nabla u|^2 \rangle$ :

$$S^+ W^+ \approx \varepsilon_K^+; \quad \varepsilon_K^+ = K^{+3/2} / [\kappa_K \ell_K^+]. \quad (5)$$

Here the dissipation is estimated via the energy cascade over scales involving a characteristic scale of energy containing eddies,  $\ell_K(z)$  determining the energy transfer rate. The constant  $\kappa_K$  will be used to ensure that the slope of this function at  $z^+ = 0$  is unity.

Note that in Eqs. (4) and (5) we used a local-balance approximation, neglecting the spatial energy flux. This approximation is very good in the log-law region but it deteriorates near the wall and near the center-line. Nevertheless for our purposes this has no consequences. Near the wall  $W^+ \ll S^+$  and the local-balance approximation plays no role in the exact mechanical balance (3) that determines  $S$ . For the same reason we also do not need to introduce a correction  $r_K(z^+)$  in Eq. (5) due to the direct viscous dissipation (similar to  $r_w(z^+)$  in Eq. (4) since the length scale replacing  $\ell_{\text{buf}}^+$  here will be the dissipative scale  $\ell_{\text{diss}} \approx 5$  which is entirely buried in the region where  $W$  and  $K$  are small. Near the centerline  $S^+$  tends to zero and Eq. (3) determines  $W^+ \approx 1 - \zeta$ , which allows an accurate determination of  $S^+$ , because we know that  $\ell_w$  and  $\ell_K$  must saturate.

**Profiles of the characteristic length-scales  $\ell_K, \ell_w$ :** Now we show that the source of confusion is the assumption that the relevant length scales can be determined *a-priori* as  $\ell_{K,w}^+ \propto (z^+)^\alpha$  with  $\alpha = 1$  or  $\alpha \neq 1$ . The actual dependence  $\ell_w$  and  $\ell_K$  on  $z$  and  $L$  can be found from the data provided by the numerical simulations. Consider first  $\ell_w$ , defined by Eq. (4). We expect that plotting the scaling function  $\ell_w^+/\text{Re}_\tau$  computed for different values of  $\text{Re}_\tau$  should collapse the data onto one scaling function. The quality of the data collapse for this scaling function is presented in Fig.2, demonstrating the expected saturation at the center-line.

The second length-scale,  $\ell_K^+$ , is determined by the second of Eq. (5). We again expect that  $\ell_K^+/\text{Re}_\tau$  should collapse the data obtained from different value of  $\text{Re}_\tau$  onto one scaling function. In Fig. 2 we demonstrate that this scaling function leads to acceptable data collapse

throughout the channel and for all the four values of  $\text{Re}_\tau$  for which the simulation data are available.

**Solution, Velocity Profiles and Final Scaling Function:** Solving Eqs. (3) together with  $S^+ W^+ = K^{+3/2} / (\kappa_K \ell_K^+)$  that follows from Eq. (5), we find

$$W^+ = (\kappa S^+ \ell^+)^2 r_w^{-3/2}, \quad (6)$$

where we have defined the von-Kàrmàn constant  $\kappa \equiv (\kappa_w^3 \kappa_K)^{1/4} \approx 0.415$  and the crucial scaling function  $\ell^+(\zeta)$  as follows

$$\ell^+ \equiv [\ell_w^+{}^3(\zeta) \ell_K^+(\zeta)]^{1/4} = \sqrt[4]{W^{+3} r_w^3 / S^{+3} \varepsilon_K^+}. \quad (7)$$

Note that if one replaces the energy dissipation rate  $\varepsilon_K^+$  by the rate of energy production  $W^+ S^+$  and takes  $r_w$  as unity this scaling function becomes the Prandtl mixing length [1]. However the latter suffers from a non-physical divergence at the center-line whereas our length saturates to a constant there as it should.

The convincing data collapse for the resulting function  $\ell^+(\zeta)/\text{Re}_\tau$  is shown in Fig. 2, rightmost panel. Substituting Eq. (6) in Eq. (3) we find a quadratic equation for  $S$  with a solution:

$$S^+ = \frac{\sqrt{1 + (1 - \zeta)[2\kappa \ell^+(\zeta)]^2 / r_w(z^+)^{3/2} - 1}}{2[\kappa \ell^+(\zeta)]^2 / r_w(z^+)^{3/2}}. \quad (8)$$

To integrate this equation and find the mean velocity profile for any value of  $\text{Re}_\tau$  we need to determine the scaling function  $\ell^+(\zeta)$  from the data. A careful analysis of the DNS data allows us to find a good *one-parameter* fit for  $\ell^+(\zeta)$

$$\frac{\ell^+(\zeta)}{\text{Re}_\tau} = \ell_s \left\{ 1 - \exp \left[ -\frac{\tilde{\zeta}}{\ell_s} \left( 1 + \frac{\tilde{\zeta}}{2\ell_s} \right) \right] \right\} \quad (9)$$

where  $\tilde{\zeta} \equiv \zeta(1 - \zeta/2)$  and  $\ell_s \approx 0.311$ . The quality of the fit is obvious from the continuous line in the rightmost panel of Fig. 2. Note that the fit function is exactly constant at mid channel, with zero slope. This is required by symmetry, and will be the reason for our excellent fit of data in the wake region.

Finally the theory for the mean velocity contains three parameters, namely  $\ell_s$  together with  $\ell_{\text{buf}}^+$  (which determines  $B$  in Eq. (1)) and  $\kappa$ . We demonstrate now that with these three parameters we can determine the mean velocity profile for any value  $\text{Re}_\tau$ , throughout the channel, including the viscous layer, the buffer sub-layer, the log-law region and the wake. Examples of the integration of Eq. (8) are shown in Fig. 1. It is worthwhile to reiterate that the excellent fits in the viscous and the wake regions (superior to the fits presented in [11, 12]), which are usually most difficult to achieve, are obtained here due to the correct asymptotics of  $\ell^+(\zeta)$  at  $\zeta \rightarrow 0$  and  $\zeta \rightarrow 1$ . In addition, our theory results also in the kinetic

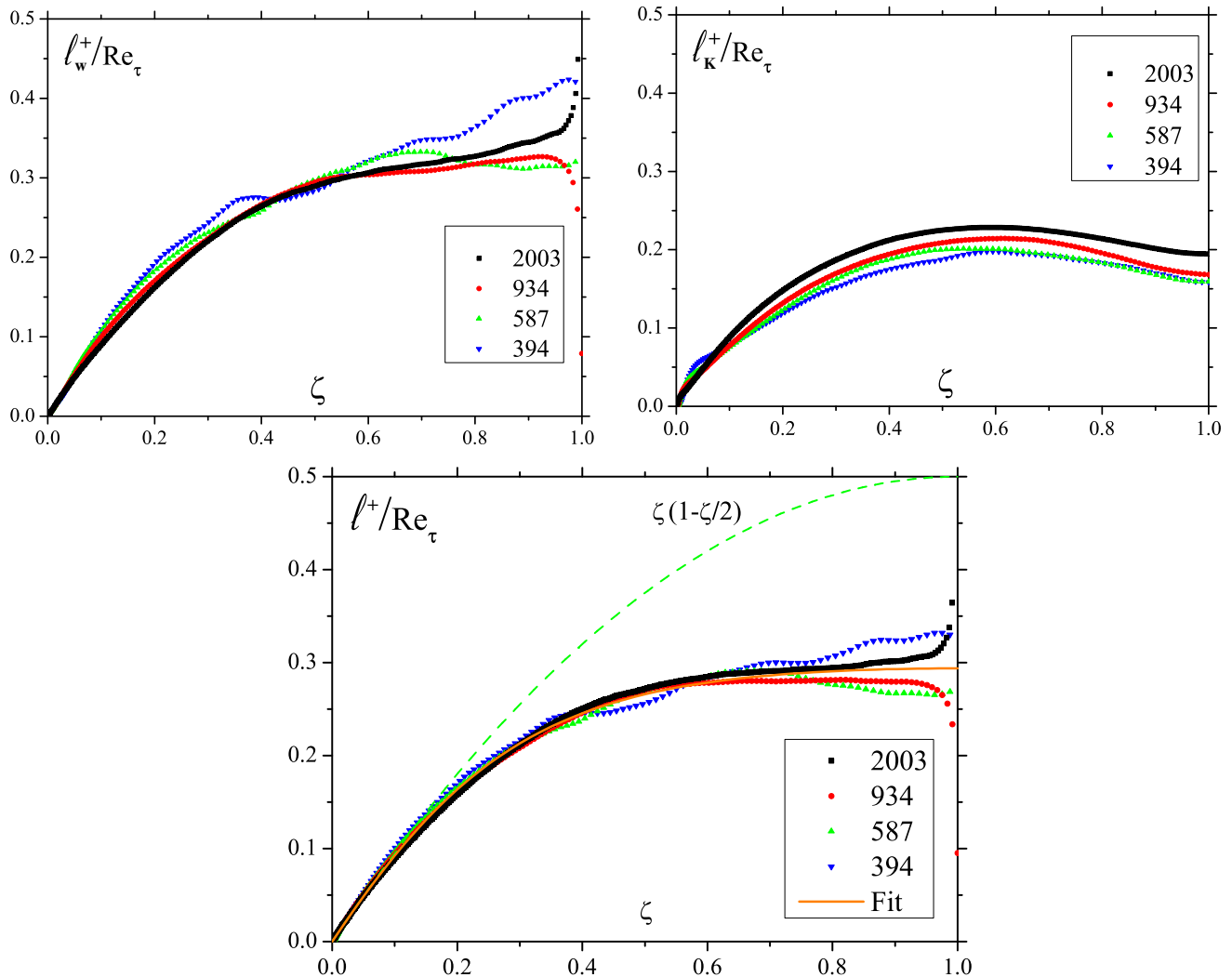


FIG. 2: Color online. The scaling function  $\ell_w^+(\zeta)/\text{Re}_\tau$  (Left upper panel),  $\ell_K^+(\zeta)/\text{Re}_\tau$  (Right upper panel) and the final scaling function  $\ell^+(\zeta)$  (Lower panel), as a function of  $\zeta \equiv z/L$ , for four different values of  $\text{Re}_\tau$ , computed from the DNS data [2, 3]. Note the data collapse everywhere except at  $\zeta \rightarrow 1$  where  $W^+ \sim S^+ \ll 1$  and accuracy is lost. The green dash line represents  $\tilde{\zeta} = \zeta(1 - \zeta/2)$  with a saturation level 0.5; in orange solid line we show the fitted function Eq. (9) with  $\ell_{\text{sat}} = 0.311$ .

energy, and Reynolds stress profiles which are in a quantitative agreement with the DNS data; for  $W$  profiles see Fig. 1.

**Conclusions and application to experiments:** We discussed turbulent channel flow, demonstrating the existence and usefulness of a scaling function  $\ell^+(\zeta)$  which allows us to get the profiles of the mean velocities for all values of  $\text{Re}_\tau$  and throughout the channel, in a good agreement with DNS. We argued that the controversy between power-laws and log-laws is moot, stemming from a rough estimate of the scaling function  $\ell^+(\zeta)$ . While this function begins near the wall as  $z^+$ , it saturates later, and its full functional dependence on  $\zeta$  is crucial for finding the correct mean velocity profiles. The approach also

allows us to delineate the accuracy of the log-law presentation, which depends on  $z^+$  and the value of  $\text{Re}_\tau$ . For asymptotically large  $\text{Re}_\tau$  the region of the log-law can be very large, but nevertheless it breaks down near the mid channel and near the buffer layer, where correction to the log-law were presented.

To show that the present approach is quite general, we apply it now to the experimental data that were at the center of the controversy [5], i.e. the Princeton University Superpipe data [4]. In Fig. 1 right panel we show the mean velocity profiles as measured in the Superpipe compared with our prediction using *the same scaling function*  $\ell^+(\zeta)$ . Note that the data spans values of  $\text{Re}_\tau$  from 5050 to 165000, and the fits with only three  $\text{Re}_\tau$ -independent

constants are very satisfactory. Note the 2% difference in the value of  $\kappa$  between the DNS and the experimental data; we do not know at this point whether this stems from inaccuracies in the DNS or the experimental data, or whether turbulent flows in different geometries have different values of  $\kappa$ . While the latter is theoretically questionable, we cannot exclude this possibility until a better understanding of how to compute  $\kappa$  from first principles is achieved.

**Acknowledgements:** We thank L. Smits for providing the data of the Princeton Superpipe and P. Monkewitz and H. Nagib for useful discussion and access to their paper prior to publication. This work is supported in part by the US-Israel Binational Science Foundation.

**Appendix:** The exact balance equation for the Reynolds shear stress can be found in [1]:  $P_w^+ + \mathcal{R}_w^+ = \varepsilon_w^+ - T_w^+$ . Here  $P_w^+ = -\tau_{yy}^+ S^+$  is the production of  $W^+$ ,  $\mathcal{R}_w^+$  is the redistribution of  $W^+$  between other Reynolds stress components,  $\varepsilon_w^+$  is the viscous dissipation of  $W^+$  and  $T_w^+$  is the turbulent transport of  $W^+$ . Explicit expressions for these terms are in [1]. Since  $\tau_{yy}$  is  $\mathcal{O}(K)$ , we approximate  $P_w^+ \propto -K^+ S^+$ .  $\mathcal{R}_w^+ = R_w^{\text{RI}+} + R_w^{\text{IP}+}$  [1, 11]. The first term describes the return to isotropy, while the second one is responsible for the isotropization of production. A slightly modified Rotta's model [13] proposes that  $R_w^{\text{RI}} \propto \sqrt{K} W / \ell_w$ .  $R_w^{\text{IP}}$  is modeled according to [1, 14], such that  $R_w^{\text{IP}} \propto K^+ S^+$ .

The viscous dissipation  $\varepsilon_w \equiv \nu \langle \partial_k u_x \partial_k u_z \rangle$  is  $\mathcal{O}(-\nu W z^{-2})$ . As explained in the text, we can neglect the non-local term  $T_w$  in the balance for the Reynolds stress with impunity. To compensate for its loss in the viscous range we increase the estimate  $(-\nu W z^{-2})$  by a factor  $\sqrt{K/K_*}$ , where  $K_*$  is a dimensional constant [11]. Eventually,  $\varepsilon_w^+ \propto -W^+ \sqrt{K^+} / z^{+2}$ . Hence, the approximate algebraic balance equation for the Reynolds shear stress reads:

$$-aK^+ S^+ + b \frac{W^+ \sqrt{K^+}}{\ell_w^+} + cK^+ S^+ \approx -d \frac{W^+ \sqrt{K^+}}{z^{+2}}, \quad (10)$$

where  $a, b, c, d$  - are positive constants of  $\mathcal{O}(1)$ . The last equation may be rearranged to the form of the fist of Eq. (4) but with  $r_w \equiv 1 + \ell_{\text{buf}}^+ \ell_w^+ / z^{+2}$ ,  $\ell_{\text{buf}}^+ \equiv d/b$ . Since

the second term is dominant only near the wall where  $\ell_w^+ = z^+$ , then  $r_w \rightarrow 1 + \ell_{\text{buf}}^+ / z^+$ . In [12] it was realized that this form, which is an interpolation between the near wall and the bulk physics, can be modeled in a way that reflects better the actual width of the buffer layer, using another interpolation formula that reads

$$r_w \equiv \left[ 1 + \left( \frac{\ell_{\text{buf}}^+}{z^+} \right)^n \right]^{1/n} \quad (11)$$

with  $n = 2$ . Best fit to simulational data which is currently available is obtained with  $5 < n < 7$ . In this Letter we chose  $n = 6$  leading to the second of Eqs. (4). This choice simplifies the appearance of the Eqs. (6)-(8).

- 
- [1] S.B. Pope, *Turbulent Flows*, 1st ed. (Cambridge University Press, 2000).
  - [2] R. G. Moser, J. Kim, and N. N. Mansour, *Phys. Fluids* **11**, 943 (1999); DNS data at <http://www.tam.uiuc.edu/Faculty/Moser/channel>
  - [3] S. Hoyas, J. Jimenez, *Phys. of Fluids*, **18**, 011702 (2006); DNS data at <http://torroja.dmt.upm.es/ftp/channels/>.
  - [4] B. J. McKeon, J. Li, W. Jiang, J. F. Morrison and A. J. Smits, *J. Fluid Mech.*, **501**, 135 (2004); The data is available at [http://gasdyn.princeton.edu/data/e248/mckeon\\_data.html](http://gasdyn.princeton.edu/data/e248/mckeon_data.html).
  - [5] G.I. Barenblatt, *J. Fluid Mech.* **249**, 513 (1993), G.I. Barenblatt and A.J. Chorin, *Phys. Fluids*, **10**, 1043 (1998),
  - [6] A.J. Smits and M.V. Zagarola, *Phy. Fluids*, **10**, 1045 (1998), M.V. Zagarola, A.E. Perry and A.J. Smits, *Phys. Fluids*, **9**, 2094 (1997).
  - [7] W. K. George, *Phil. Trans. R. Soc. A* **365**, 789 (2007)
  - [8] R. L. Panton, *Phil. Trans. R. Soc. A* **365**, 733 (2007)
  - [9] P. Monkewitz, K. A. Chauhan, H. M. Nagib, submitted to *Phys. Fluids*.
  - [10] J. Boussinesq, *Theorie de l'ecoulement tourbillant*. Mem. Pres. Acad. Sci. XXIII, 46, Paris, 1877.
  - [11] V. S. L'vov, I. Procaccia and O. Rudenko, *JETP Letts*, **84**, 67-72 (2006);
  - [12] V.S. L'vov, A. Pomyalov, I. Procaccia and S.S. Zilitinkevich, *Phys. Rev. E.*, **73**, 016303 (2006).
  - [13] J.C. Rotta, *Z. Phys.* **129**, 547 (1951).
  - [14] D.A Naot, A. Shavit, and M. Wolfshtein, *Israel J. Technol.* **8**, 259 (1970).